Mathematical Biosciences 308 (2019) 42–58

Contents lists available at ScienceDirect

Mathematical Biosciences

journal homepage: www.elsevier.com/locate/mbs

Modeling the interactions among phythopatogens and phyllosphere microorganisms for the biological disease control of *Olea europaea* L.

Paula Baptista[a], Iulia Martina Bulai[*,1,b], Teresa Gomes[a], Ezio Venturino[1,c]

[a] CIMO, School of Agriculture, Polytechnic Institute of Bragança, Campus de Santa Apolónia, Bragança 5300-253, Portugal
[b] Department of Information Engineering, University of Padova. Via Gradenigo, 6/B, 35131, Padova, Italy
[c] Dipartimento di Matematica "Giuseppe Peano" Università di Torino, via Carlo Alberto 10, Torino 10123, Italia

ARTICLE INFO

Keywords:
Olive tree disease
Mathematical model
Bistability
Oscillating behavior

ABSTRACT

In this paper we formulate a model for assessing the interaction between the phytopathogen *Spilocaea oleaginea* and the phyllosphere microorganisms that are present in the olive tree leaves. The model describes the evolution in time of the foliage of the olive tree and the two different microorganisms, the phytopathogen fungi, that negatively affect the plant causing spots in the leaves, and the beneficial phyllosphere microorganisms, that help in keeping in check the invasion of the former. The system possesses five equilibria that are suitably analysed for feasibility and stability. The model shows interesting features: a bistable behavior, exhibited by three different pairs of equilibria. The separatrix surface of the basins of attraction of one such pair is computed. This allows the possible assessment of human intervention for control of the disease. Persistent oscillations via Hopf bifurcation are also discovered.

1. Introduction

The olive tree (*Olea europaea* L.) has a great economic importance in the Mediterranean region [1]. This has been relevant all throughout history since very ancient times, dating back up to at least the classical Greek civilisation [2].

This plant however may be subject to several diseases that can hinder its growth, reducing the olives production and even cause its death [3]. These facts entail considerable economic losses for the farmers. The main diseases that affect olive trees are mostly caused by fungi and bacteria, which can infect several parts of the plant (roots, stem, fruits and leaves) [3]. Nowadays, olive diseases control programs rely mostly on chemical control by application of copper-based fungicides [3]. Besides having limited efficacy, this control measure is not compatible with sustainable production systems (organic and integrated production) which are the pillars of the European Model for Agriculture, according the Directive 2009/128/EC. In olives production, the plant protection strategy must follow the Guidelines for integrated production of olives [4]. Thus, a need to develop novel and environment-friendly control strategies for the biological management of olive diseases has recently become an important issue, involving both biological issues as well as applied mathematics concepts and is leading to an interesting research topic.

The aerial parts of the olive plants (phyllosphere) are colonized by a diverse microbial community (mostly bacteria and filamentous fungi), which can grow both epiphytically on the surface of plant tissues and endophytically within the tissues [5]. These microorganisms interact with each other and with the host plant, mediating several ecosystem processes by altering plant traits [6], including disease resistance traits [7]. Phyllosphere microorganisms can reduce the infection of plant tissues by pathogens either directly, through the production of antagonistic molecules and competition for resources, or indirectly by induction of plant resistance response [8]. Because of the importance of the microbiome for host fitness and function, there is a growing desire to model and manage host-microbiome interactions [9], to improve crop yields [10,11]. In this way, the development of the so-called "microbiome-driven cropping systems" might result in the next revolution in agriculture, resulting in a more sustainable system for plant production [10,11].

Phyllosphere-associated microorganisms may be explored, in an integrative perspective, for designing new strategies for the biological control of olive diseases. Indeed, in the laboratory the salient components of the antagonistic molecules of these microorganisms can be artificially produced and then sprayed on the infected trees, to control the infection. However, the assessment of the impact that such possible strategies have on the cultures cannot be evaluated easily in the field.

* Corresponding author.
E-mail addresses: pbaptista@ipb.pt (P. Baptista), iuliam@live.it (I.M. Bulai), ezio.venturino@unito.it (E. Venturino).
[1] Member of the research group GNCS of INdAM.

https://doi.org/10.1016/j.mbs.2018.12.002
Received 29 May 2018; Received in revised form 4 September 2018; Accepted 3 December 2018
Available online 04 December 2018
0025-5564/

This kind of assay requires artificial inoculation of olive tree leaves with the pathogen *Spilocaea oleaginea* (syn. *Venturia oleaginea*) and with the "good" native fungi. Several explanations for the difficulty in studying such microbial interactions in the phyllosphere may be considered. One is related to the pathogen which is a recalcitrant fungus to manipulate due to the difficulty in culturing it, and additionally shows also a slow growth rate. A second explanation is related to the complexity of the microorganisms that inhabit the phyllosphere. Not only their identity remains largely unknown, but in particular their adaptations to the habitat and their potential role with respect to modulating population sizes of pathogens. Moreover, most of the microorganisms existing on plant leaves are uncultivated, a fact which can jeopardize plant inoculations. Last but not least, the olive tree used in the assays must be sterile (not colonized by microorganisms), which is impossible to obtain in nature. Taken together, these challenges mean that a comprehensive field analysis of interactions between pathogen and "good" fungi in the olive tree leaves is far from being trivial. Hence, it is effectively impossible to design an experimental approach that can validate it. Nevertheless, even some partial information on such kind of topic may be of relevance for plant health, giving the farmers a way of preventing foliar fungal pathogens. Thus, the response provided by the mathematical model developed in this work represents an elegant way of describing interactions between the pathogen and beneficial fungi that would otherwise be very difficult to demonstrate on real leaf surfaces. We further remind the reader that, generally, in ecological terms, experiments performed for e.g. one year, provide in general just a few measurements for the relevant parameters sought. To obtain a statistically significant sample of values may require in some instances even decades.

This of course implies also an extremely high cost for carrying out these experiments.

Thus the need of an alternative approach is evident. In this respect, mathematical modeling may help in conducting in-silico experiments. The computer replaces the environment, while showing the behavior in time of an ecosystem suitably modeled via a set of differential equations.

In this work, the potential role played by phyllosphere microorganisms in the protection of host olive trees from phytopathogen infection is explored. This involves both situations of the phyllosphere microorganisms seen as direct biological control agents or through their management in order to reduce phytopathogens.

The paper is organized as follows. In the next section we present the mathematical model. The possible ecosystem outcomes are explored and discussed in Section 3. Then, numerical simulations are carried out, outlining interesting features of the possible ecosystem configurations. A final discussion of the results obtained concludes the paper.

2. The model

Specific models for tree and crop pathogens and their induced disease propagation are present in the literature, see for instance [14,21], addressing either the disease itself [12] and the ways for its possible control [13], their influence on crops and possible alternative cultivation ways to curbe them [15]. A specific example of a fungus heavily affecting vineyards is in particular considered in [16].

We consider a single olive tree that is affected by a disease caused by fungi, identified as the "bad" fungi from now on. We assume that among the phyllosphere microorganisms on the olive tree there is present another type of fungi, called the "good" ones, that have a double positive effect.

Good fungi control plant diseases caused by pathogenic fungi directly by antibiosis, mycoparasitism and competition for space and nutrients, thereby removing them from the environment and the tree's canopy. In doing so they also obtain a reward, gaining more space and more food directly from the plant. Secondly, they are bioprotectant for the tree, exerting on it a further direct beneficial effect. Therefore these two types of fungi and the tree are linked by complex mutual interactions that are both of competition or predator-prey type, as well as of symbiotic nature. The purpose of our model is the elucidation of the role that these interactions play for the whole tree health, and possible ways for improving it. Therefore, even though this may somewhat complicate the shape of the resulting dynamical system, we want to consider all the possible interactions that may occur among the selected ecosystem variables because of the several possible ways of influencing each other.

The four populations (all measurable by biomass or extent of surface) that are taken into account in the ecosystem are

- S: the healthy branches and leaves of the olive tree.
- I: the branches and leaves of the same olive tree that are infected by the pathogenic fungi. We assume that the infected branches and leaves do not reproduce.
- F: the pathogenic filamentous fungi, attacking and infecting the olive branches and leaves. This is a fundamental variable in the system, that must be taken into account, because it is responsible for the infection process. Since it has in general a negative effect on the ecosystem, to simplify the model formulation, one may at first think to replace it by a kind of "harvesting" term in the relevant equation, which has for the corresponding dependent variable the same detrimental effect. But in this way the possible outgrowth of these pathogens would be completely omitted in the model description, and therefore the model from the start would not be able to shed any light on biological ways of keeping these pathogens in check.
- G: the phyllosphere microorganisms; they essentially remove the F's, benefiting then by getting more space for their growth and more food directly from the plant, with this behavior they also further contribute directly to the benefit of the healthy parts of the plant, S. This variable is also relevant, because, as previously illustrated, if its role in the ecosystem is clarified, a kind of "artificial" antagonistic molecules could be produced in the laboratory and then used on the cultures.

The model reads:

$$\begin{aligned}
\frac{dS}{dt} &= s\left(1-\frac{S+I}{K}\right)S - \lambda SF + bGS\\
\frac{dI}{dt} &= \lambda SF - gI - qIF - s\frac{S+I}{K}I\\
\frac{dF}{dt} &= hqIF - aGF - mF - rF^2 - gIF_{av} - s\frac{S+I}{K}IF_{av}, \quad F_{av} = \frac{F}{I}\\
\frac{dG}{dt} &= ebGS + uaGF - nG - pG^2 - gIG_{av} - s\frac{S+I}{K}(S+I)G_{av},\\
& \qquad G_{av} = \frac{G}{S+I}.
\end{aligned} \tag{1}$$

In the first equation the evolution of healthy leaves is described. They reproduce following a logistic growth, with net reproduction rate s and carrying capacity K. They may become infected at rate λ by the action of the bad fungi, whose spores are transported by wind and rain to all parts of the tree, assuming well mixing. Finally they get benefit at rate b from the good fungi, that are their bioprotectants as stated above. In fact this term, coupled with a similar one that appears in the last equation, indicates the symbiotic relationship existing between healthy branches and good fungi, which will also be studied more at depth when the specific submodel will be investigated.

The second equation for the infected leaves shows that they become so when they are attacked at rate λ by the bad fungi. As for the remaining terms, recall that we want to consider all possible interactions that may occur among the ecosystem variables. When, as is in this specific case, all of them are detrimental for the population in consideration, they act as additional deaths for it. It is true that then, they could in principle be conglobated into just one single mortality term,

simplifying the model formulation, but in this way the mutual population influences would be missed. Thus, despite the complications, we prefer to deal with this more elaborated version of the model. The infected leaves experience natural mortality at rate g. When infected by the pathogenic fungi F's, the infected leaves' abundance is reduced at rate q, which constitutes an additional, disease-related, mortality, and also are subject to intraspecific competition because the healthy and infected olive leaves and branches subtract resources to I's, at rate sK^{-1}. Note that introducing intraspecific competition among these infected leaves allows something more. Indeed note that defining the total leaves of the tree, $L = S + I$, by summing the first two equations in the system (1), one obtains a basic logistic growth for the canopy L, in which the effects of the microorganisms and of the infection are also accounted for, namely

$$\begin{aligned}\frac{dL}{dt} &= s(L-I) - \frac{s}{K}L^2 + bG(L-I) - qIF - gI \\ &= s\left(1-\frac{L}{K}\right)L + bGL - (qF + b + g + s)I.\end{aligned}$$

In the third equation we model the pathogenic filamentous fungi. Here there are more relationships to be taken into account, that complicate the formulation. In particular the adverse mechanisms against these agents should all be considered, as they would perhaps provide key elements for their control. Natural and intraspecific competition are the basic elements, to which the antagonistic effects must be added. Finally, because the infected tree loses the diseased leaves, we should also account for the fact that the fungi on those leaves disappear from the tree as well. To be more specific, consider each term in the equation, as follows. The pathogens extract nutrients from the infected leaves, as already mentioned at rate q, with a conversion factor h. They die because they are killed by the good fungi, at rate a, and also naturally at rate m, possibly very very small. Bad fungi can die also by intraspecific competition, at rate r. In addition, they are removed from the foliage when the leave dies and falls via disease-related, mortality and also by the intraspecific competition with other leaves. Note however that when the leave falls, it carries with it an average content of fungi denoted by F_{av}. Because the leave falls when it dies, we find the two mortality terms appearing in the second equation for infected leaves in this equation for fungi as well. Note that the term in q that in the equation for the infected parts of the tree represents a hindering of the leaves growth, is not accounted here as a mortality for the bad fungi, but rather it is the benefit they get from the leaves, contributing positively to the F's growth, as said above. Indeed it represents their gain in energy by nutrients extraction from the leaves.

The good fungi in the phyllosphere are modeled in the fourth equation. We stress again that the aim of this study is the clarification of the relationships among all the system variables. Therefore one should once more expect that this equation, as well as the former one, is rather complicated, in view of their rewarding interactions of the good phyllosphere organisms with healthy branches and bad fungi, as well as to the detrimental one due to natural deaths and intraspecific competition, and to their loss when the leaves on which they thrive drop. They get food from their beneficial relationship with the healthy leaves, at rate b, scaled by the conversion factor e, and also by killing the bad fungi at rate a. In this way they have two types of benefit, directly getting more space for their growth, and also more food. Here u represents another conversion factor. Good fungi also die naturally at rate n and experience intraspecific competition at rate p as well. In the last two terms, we model the fact that they also are removed from the foliage when an infected leave dies and falls, if they happen to be on it. This mortality could be induced by the action of the bad fungi, firth term, but also by the leaves' intraspecific competition, last term. Here G_{av} stands for the average content of the good fungi on a leave. Note indeed that good fungi are present both on infected and healthy plant units. As it occurs for the equation of bad fungi, we find the two mortality terms appearing in the second equation for infected leaves to appear in this one also, when the leave falls, i.e. when it dies. Similarly as for the third equation, we do not account among the mortalities the term in q appearing in the second equation for infected leaves, because it represents the process of extracting nutrients from the F's as said above and does not therefore represent a real mortality for the leaves, but only their damage due to F's.

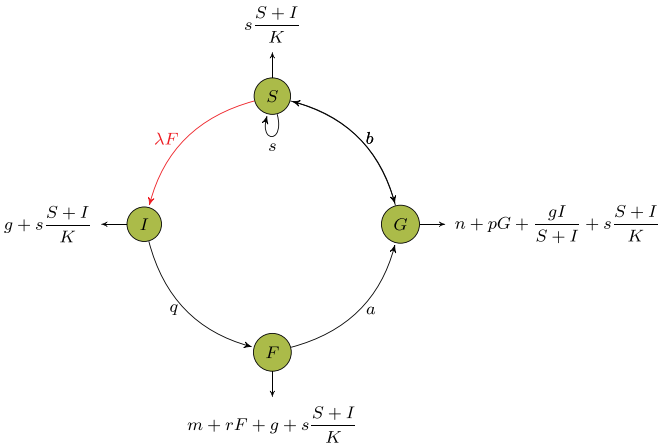

Fig. 1. Schematic representation of the ecosystem relations, with the notation referring to model (2).

Substituting $F_{av} = FI^{-1}$ and $G_{av} = G(S+I)^{-1}$ in the last two equations of the system (1), after simplifications the model becomes

$$\begin{aligned}\frac{dS}{dt} &= s\left(1-\frac{S+I}{K}\right)S - \lambda SF + bGS \\ \frac{dI}{dt} &= \lambda SF - qIF - gI - s\frac{S+I}{K}I \\ \frac{dF}{dt} &= hqIF - aGF - mF - rF^2 - gF - s\frac{S+I}{K}F \\ \frac{dG}{dt} &= ebGS + uaGF - nG - pG^2 - gI\frac{G}{S+I} - s\frac{S+I}{K}G.\end{aligned} \tag{2}$$

For this final model, we provide in Fig. 1 a sketch of the ecosystem, to illustrate the mutual relationships among these populations. The arrows mean that the population at the root is negatively affected by the interaction with the population that is at the head of it, which instead receives a benefit. Outgoing arrows denote losses, essentially due to deaths, either intrinsic or essentially due to competition or predation, if depending from another population. To each arrow one or more parameter are associated, describing the rate at which the underlying interaction occurs. In red is depicted the arc that is related to the infection process.

3. Ecosystem's steady states

For a deeper understanding of the full model (*S, I, F, G*) we will start by analysing the two particular cases: the disease-free model (*S, G*) and the phyllosphere microorganisms-free model (*S, I, F*) respectively.

3.1. The disease-free subsystem

From model (2) one can get the disease-free model (*S, G*)

$$\begin{aligned}\frac{dS}{dt} &= s\left(1-\frac{S}{K}\right)S + bGS \\ \frac{dG}{dt} &= ebGS - nG - pG^2 - s\frac{S}{K}G.\end{aligned} \tag{3}$$

Here we characterize all the possible steady state system's outcomes, deferring to the Appendix A the mathematical details. The results of the dynamical system analysis of (3) are:

- The trivial equilibrium point $E_0 = (0, 0)$ is always feasible but unstable.
- The good fungi-free point $E_1 = (K, 0)$ is always feasible and is stable if the carrying capacity of S is suitably bounded from above,

$$K < \frac{n+s}{be}. \tag{4}$$

Note that the higher the benefit the phyllosphere microorganisms get from the tree, parameters b and e, the lower the bound is, and conversely the larger their mortality n and the net reproduction rate s are, the larger the bound.

- The coexistence equilibrium (for this model), i.e. the point where the tree is healthy and only the phyllosphere microorganisms thrive in it,

$$E_2 = \left(\frac{K(bn-ps)}{Kb^2e-bs-ps}, \frac{s(n+s-bKe)}{Kb^2e-bs-ps}\right), \tag{5}$$

is feasible if either one of the two alternative sets:

$$b(n+s) \le b^2eK \le s(b+p); \tag{6}$$

$$b(n+s) \ge b^2eK \ge s(b+p). \tag{7}$$

Stability of this equilibrium is easily established, reducing just to the condition

$$Kb^2e < s(p+b), \tag{8}$$

which shows that it is always stable only in case of the feasibility conditions (6), as they are the only ones compatible with (8). Thus, whenever it is feasible, E_2 is always stable.

Remark 1. Note that (6) are easily seen to be the necessary conditions for which the two nullclines meet; in the opposite case, (7), the trajectories of the symbiotic system would diverge to infinity. Thus (8) rules out possible unbounded solutions of this subsystem.

3.2. The phyllosphere microorganisms-free subsystem

From the general model (2) the phyllosphere microorganisms-free model (S, I, F) can be obtained

$$\begin{aligned}
\frac{dS}{dt} &= s\left(1-\frac{S+I}{K}\right)S - \lambda SF \\
\frac{dI}{dt} &= \lambda SF - qIF - gI - s\frac{S+I}{K}I \\
\frac{dF}{dt} &= hqIF - mF - rF^2 - gF - s\frac{S+I}{K}F.
\end{aligned} \tag{9}$$

We now sum up the main results of the steady states of model (9) and analyze their stability . For the analytical results see Appendix B. The results of the dynamical system analysis are:

- The result for the trivial equilibrium E_0 is the same as for the disease-free model (3), namely unconditional instability.
- E_1 exists also in this case but here it is always stable.
- Again there is the coexistence equilibrium (in which the phyllosphere microorganisms are absent, though)

$$E_3 = \left[\frac{K}{s}\left(s - \frac{s}{K}I_3 - \lambda F_3\right), \frac{m+g+s+(r-\lambda)F_3}{hq}, F_3\right] \tag{10}$$

where F_3 is the positive root of a quadratic equation, see Proposition 2 in Appendix B, so that there can be none at all, in which case E_3 would not exist, or either one or two. Further feasibility conditions come from the nonnegativity of the remaining populations, $S_3 \ge 0$, $I_3 \ge 0$. Combined, they extensively read

$$0 \le (m+g+s) + (r-\lambda)F_3 \le \frac{hqK}{s}(s-\lambda F_3) \tag{11}$$

and in turn imply further restrictions on the size of the bad fungi. Necessarily, from the nonnegativity requirements of (11), we must have for $\lambda < r$

$$F_3 \le \frac{s}{\lambda} \tag{12}$$

for $\lambda > r$ instead

$$F_3 \le \min\left\{\frac{s}{\lambda}, \frac{m+g+s}{\lambda-r}\right\}. \tag{13}$$

But also from the right inequality in (11) it follows

$$s(m+g+s-hqK) \le (s\lambda - sr - hqK\lambda)F_3$$

which is always satisfied for

$$m+g+s \le hqK, \quad s\lambda \ge sr + hqK\lambda \tag{14}$$

while conversely it gives two more conditions on the size of F_3, respectively

$$m+g+s \le hqK, \quad s\lambda \le sr + hqK\lambda, \quad F_3 \le \frac{s(m+g+s-hqK)}{s\lambda - sr - hqK\lambda} \tag{15}$$

and

$$m+g+s \ge hqK, \quad s\lambda \ge sr + hqK\lambda, \quad F_3 \ge \frac{s(m+g+s-hqK)}{s\lambda - sr - hqK\lambda} \tag{16}$$

For the stability of E_3 the Routh–Hurwitz criterion must hold, but it is quite complicated, for more details see Appendix B.

Remark 2. This seems to be a rather interesting result, as it shows that even when it is endemically infected, a tree cannot support more than a maximal quantity of pathogens. Once more, if F were not taken as a system variable, this remark probably would have escaped the investigation.

3.3. The complete system

The equilibria found for models (3) and (9) are so also in this case for the system (2). In particular the origin continues to be always unstable, while the healthy-tree-only E_1 and the disease-free E_2 points remain unconditionally stable in this larger phase space. The infected tree situation E_3, instead, in this case possesses an additional eigenvalue that produces the following additional stability condition

$$ebS_3 + uaF_3 < n + g\frac{I_3}{S_3+I_3} + s\frac{S_3+I_3}{K}. \tag{17}$$

Thus the introduction of the “good fungi” may destabilize the endemic equilibrium, a positive effect, and might render the tree disease-free, if E_3 becomes unstable and trajectories tend then to E_1 or E_2. The disease would remain endemic instead if they approach the coexistence equilibrium.

Remark 3. Once again this result stresses the importance of considering among the ecosystem variables also the good phyllosphere antagonists, as it is seen, even analytically, that they can fight back the tree infestation by pathogens. This points out also the fact that artificial measures like spraying the synthesized antagonistic molecules can help the natural phyllosphere fungi in their task.

The disease endemicity in the general model (2) is also a possible outcome, with all the ecosystem populations thriving,

$$E_* = \left(S_*, I_*, F_*, \frac{F_*K\lambda + I_*s - Ks + S_*s}{Kb}\right),$$

with

$$G_* = \frac{F_*K\lambda + I_*s - Ks + S_*s}{Kb}, \tag{18}$$

$$F_* = \frac{I_*Kbhq - I_*as - I_*bs + Kas - Kbg - Kbm - S_*as - S_*bs}{(a\lambda + br)K}, \tag{19}$$

and where S_* and I_* are the positive coordinates of the intersection point between the curves $H(S, I)$ and $M(S, I)$, defined in Appendix C. Here the stability is ensured by the Routh–Hurwitz conditions (C.2) that are quite involved to be made explicit. For more details see Appendix C.

4. Numerical simulations

In all simulations for the system (2) the intrinsic ode45 routine of Matlab2016a is used. We found interesting dynamics that can arise, and report our results according to these features: bistability phenomena and transcritical bifurcations. We then investigate the sensitivity of the system with respect of some relevant model parameters. In doing so, Hopf bifurcations are also discovered around the coexistence states of the $S - I - F$ submodel and of the whole ecosystem, which are hard to be shown analytically, as observed in analysing the stability of these equilibria in the previous section.

4.1. Bistability configurations

Our numerical simulations show that for chosen set of parameters two different possible system's outcomes exist, if the initial conditions are suitably chosen. In particular the following pairs of bistable equilibria are found: E_1 and E^*, E_2 and E_3, E_1 and E_2.

More specifically, for the set of hypothetical parameters

$$\begin{aligned} &s = 4.1, \quad \lambda = 8.5, \quad b = 7.0, \quad q = 9.9, \quad g = 0.1, \quad h = 0.9, \\ &m = 0.3, \\ &a = 8.2, \quad e = 0.05, \quad u = 0.6, \quad n = 0.6, \quad K = 6.8, \quad r = 9.6, \\ &p = 6.9 \end{aligned} \tag{20}$$

and the initial conditions [0.01, 0.4, 0.8, 0.6] and [0.7, 0.5, 0.7, 0.6] we respectively get the two stable equilibria

$$E_1 = [6.8, 0.0, 0.0, 0.0] \quad \text{and} \quad E^* = [1.2, 0.8, 0.4, 0.1].$$

Instead, setting $g = 1$ in the above same set of parameters (20), with the initial conditions [0.01, 0.4, 0.8, 0.6] and [3, 2, 0.5, 0] the system respectively sets to the stable points

$$E_1 = [6.8, 0.0, 0.0, 0.0] \quad \text{and} \quad E_3 = [1.1, 0.6, 0.3, 0.0].$$

In Fig. 2 the trajectories converging to E_1 and E_3 are visually represented in the phase space.

For the following set of hypothetical parameter values

$$\begin{aligned} &s = 1.5, \quad \lambda = 2.7, \quad b = 2.3, \quad q = 5.9, \quad g = 0.1, \quad h = 0.8, \\ &m = 0.4, \\ &a = 2.1, \quad e = 0.2, \quad u = 0.3, \quad n = 1.7, \quad K = 8.6, \quad r = 6.1, \\ &p = 7.7 \end{aligned} \tag{21}$$

and the initial conditions [3, 2, 0.5, 0] and [3, 0, 0, 2] the stable equilibria are instead achieved

$$E_3 = [1.1, 0.6, 0.3, 0.0] \quad \text{and} \quad E_2 = [40.9, 0.0, 0.0, 2.4].$$

Remark 4. Looking at the above pairs of points, it thus appears that the system can always attain a disease-free equilibrium, at E_1, or the phyllosphere microorganisms-free point E_3, or instead settle at an endemic state. The outcome is regulated only by the present state of the system, namely the initial conditions. It becomes very much important indeed to be able to assess whether the latter will lead to disease eradication or not. This issue has been dealt with also in other similar circumstances and accurate and state-of-the-art approximation theoretic tools have been devised to assess the basins of attraction of each equilibrium of the dynamical system, [17–20]. Using these algorithms, in Fig. 3, we show the surface that separates the basins of attraction of E_1 and of E_2.

This information is useful for the administration of the ecological situation, in that it may provide guidelines on how to act on the system in order to push it into the domain in which it will naturally settle to the disease-free equilibrium.

4.2. Transcritical bifurcations

We further investigate the transition of one equilibrium into a different one by a smooth change of one or more system parameters. In Fig. 4 the transcritical bifurcation that arises varying the parameter $\lambda \in [0, 30]$ is seen, using the same set of parameters (20) and the initial conditions [1, 1, 1, 1]. For $\lambda \in [0, 5]$ the system sets to the healthy tree equilibrium configuration E_1, in the range $\lambda \in (5, 19]$, it achieves coexistence E^* and finally for $\lambda \in (19, 30]$ the phyllosphere microorganisms-free point E_2 is attained.

Fig. 5 shows instead the transcritical bifurcation arising by varying the parameter $\lambda \in [0, 30]$, using the same set of parameters (21) and the initial condition [1, 1, 1, 1]. For $\lambda \in [0, 3] \cup (10, 30]$ the system achieves the disease-free equilibrium E_2, while for $\lambda \in (3, 10]$, it settles to E_3.

Remark 5. In this context it is thus apparent that a lower disease transmission rate helps in keeping the disease in check. This remark may be useful in the context of climatic changes, since the disease transmission rate λ might be dependent on external factors, in particular might increase with a raise of the environmental temperature.

4.3. Equilibria sensitivity to two parameters variations

So far we have analysed the behavior of the equilibrium points keeping the parameters fixed, while changing the initial conditions. We discovered bistability among at least tree pairs of equilibria, in one case also plotting the separatrix surface, Fig. 3. We now investigate the question of what happens to the ecosystem instead if pairs of model parameters change. We thus analyse the behavior of the populations when two of the parameters are simultaneously varying. At first we consider the three pairs of parameters: (g, λ), (g, b) and (λ, b), because these are ecologically the most relevant. Indeed, g represents the natural mortality rate of the infected parts of the olive tree, but extending the interpretation it can also be seen as an external human action on the ecosystem, the pruning of the infected parts of the tree; λ is the infection rate, that may well be temperature-dependent and b represents the mutual benefit between phyllosphere microorganisms and the olive tree. In addition, these pairs of parameters also give the most significant results.

For the set of parameters (21) varying the parameters $g \in [0.1, 4]$ and $\lambda \in [0.1, 11]$, and with the initial conditions [1, 1, 1, 1] the system outcomes are shown in Fig. 6.

As it is apparent from Fig. 6, I and F vanish if g is larger than a certain threshold, in which case the stable disease-free point E_2 is

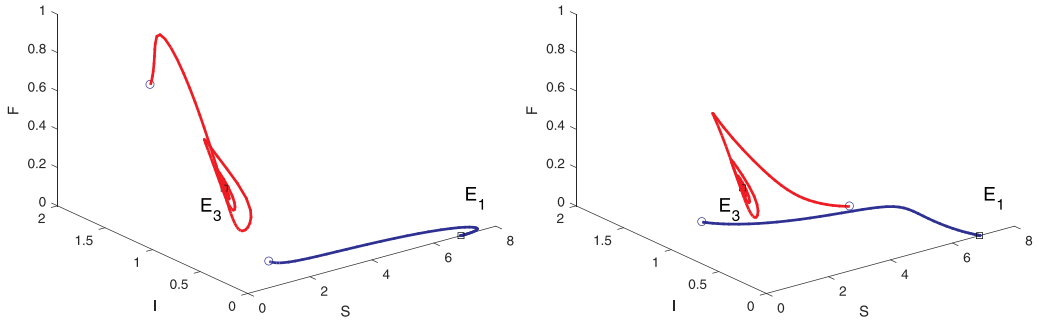

Fig. 2. In the subspace $G = 0$ of the phase space we represent the projections of two different trajectories converging to E_1 and E_3 respectively. Blue dots: the initial conditions, [1, 0.1, 0.1, 1] and [3, 0.3, 1, 1], for the right frame and [1, 0.1, 0.1, 1] and [0.3, 0.3, 1, 1], for the left frame; Black squares: the stable equilibrium points to which the trajectories tend; they respectively are $E_1 = [6.8, 0, 0, 0]$ and $E_3 = [1.1, 0.6, 0.3, 0]$. Blue line: the trajectory tending to E_1; Red line: the trajectory tending to E_3. (For interpretation of the references to color in this figure legend, the reader is referred to the web version of this article.)

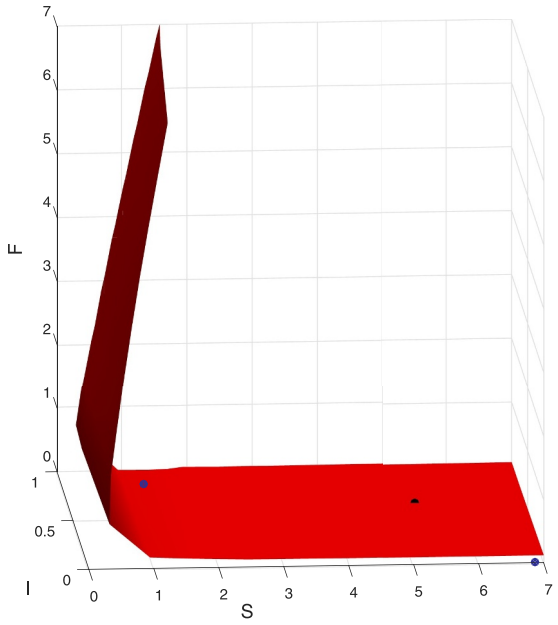

Fig. 3. In the $G = 0$ subspace of the phase space, we represent the projection of the separatrix hypersurface partitioning the phase space into the basin of attraction of $E_1 = [6.8, 0.0, 0.0, 0.0]$, on the left and below it and the one of $E_3 = [1.1, 0.6, 0.3, 0.0]$, lying instead above it and to its right. The two equilibria are indicated with blue dots. (For interpretation of the references to color in this figure legend, the reader is referred to the web version of this article.)

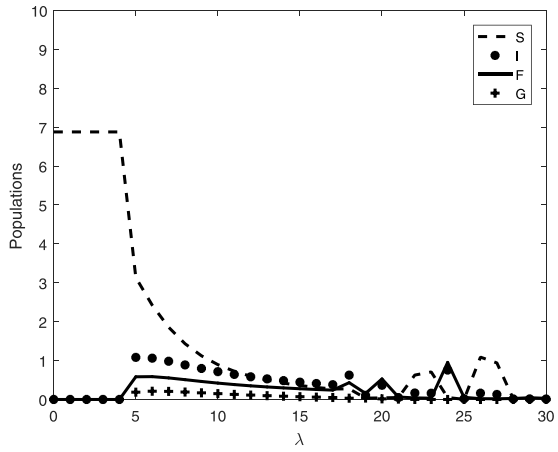

Fig. 4. The transcritical bifurcation bringing the ecosystem from the equilibrium E_1 to the coexistence point E^* and finally to E_2, varying $\lambda \in [0, 30]$. The initial condition used is [1, 1, 1, 1].

attained. There is a kind of semicircular region for $2 \lesssim \lambda \lesssim 3$ where the infection is endemic, while the healthy parts of the tree and the phyllosphere microorganisms settle to very low values.

For the set of parameters (20) varying the parameters $g \in [0.1, 4]$ and $b \in [0.1, 15]$, and with the initial conditions [1, 1, 1, 1] the results appear in Fig. 7.

Keeping for the time being a fixed value of b, it can be seen from Fig. 7 that for $g \lesssim 0.5$ the four populations coexist, E^*. In the range $g \gtrsim 1.5$ only the healthy parts of the tree S survive at carrying capacity, E_1. Increasing b, for $g \lesssim 0.5$, the system populations S, I, F and G all increase.

Remark 6. This result is relevant, because it shows that a high filamentous fungi mortality rate, natural or human induced via pruning, induces the recovery of the plants, almost independently of the disease transmission rate.

Again, for the set of parameters (20) but this time varying the pair of parameters $\lambda \in [0.1, 4]$ and $b \in [0.1, 15]$, and with the initial condition [1, 1, 1, 1], Fig. 8 contains the simulations results.

The pictures in Fig. 8 are almost independent of the value of b, with the exception that an increase in the latter is beneficial for the phyllosphere microorganisms. For $\lambda \lesssim 4$ we get the disease-free equilibrium E_1, in the range $4 \lesssim \lambda \lesssim 22$ the system attains coexistence, but for λ past a certain value, around 15, oscillations are triggered via a Hopf bifurcation. The two surfaces in each frame represent respectively the minimum and the maximum values of the oscillating solutions.

From Fig. 9, the results in the parameter space (λ, a) are similar as those obtained for (λ, b), with the only difference that for small values of a the phyllosphere microorganisms-free point is stable. For large values of a instead the same behavior is exhibited as in Fig. 8.

Fig. 10 shows that varying n together with λ does not affect any population except for the phyllosphere microorganisms, that vanish for a high enough n. Thus the intrinsic mortality rate of phyllosphere microorganisms cannot help in fighting the disease; rather, a high n compromises their survival, as it should be expected. The limit cycles are once more found for a large disease contact rate λ.

Fig. 11 contains the simulations in the (r, λ) parameter space: combinations of large λ and low r or low λ and high values of r also entail disease eradication. The parameter r represents the intraspecific competition among filamentous fungi and is therefore an intrinsic

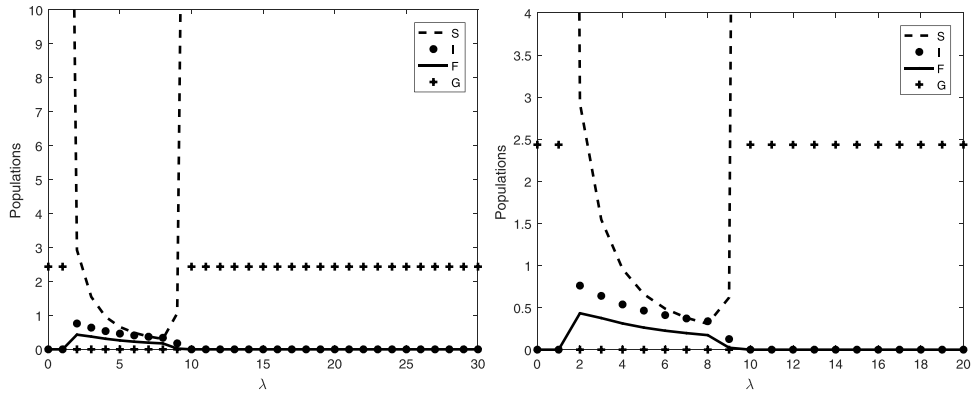

Fig. 5. Left frame: The transcritical bifurcation taking the system from E_2 to E_3 and then finally to E_2. It is obtained by varying $\lambda \in [0, 30]$. The initial condition is [1, 1, 1, 1]. Right frame: the zoomed version to better illustrate the details for low values of λ.

parameter of the ecosystem. In this case, to act on it via external measures might perhaps be a bit of a problem. Hence this result is most likely not practically usable.

Further, Fig. 12 shows the system behavior in the (q, λ) parameter space. Even for highly transmissible infection, large λ it would be possible to eradicate the disease if q, the feeding rate of filamentous fungi on infected leaves, can be kept at very low values. This perhaps might be enhanced by some external measures, possibly to be devised ad hoc.

Finally in Fig. 13 we graphically illustrate the onset of sustained oscillations for the set of suitably chosen parameters: $s = 3.5$, $\lambda = 9$, $b = 5.4$, $q = 8.3$, $g = 0.8$, $h = 0.9$, $m = 0.05$, $a = 7.8$, $e = 0.2$, $u = 0.1$, $n = 4.6$, $K = 9.1$, $r = 5.5$, $p = 5.8$.

In order to better understand the ecosystem behavior, we have checked for each set of parameter values whether the surface represented in the previous pictures corresponds or not to a single stable equilibrium point. Thus we ran simulations fixing the parameter at the values used to generate the surface, and fixing the two parameters that appear in the domain of each surface to their mean value, i.e. at the center of the rectangle in the domain of the surface. Then we took 50 randomly generated initial conditions, in the hypercube with center given by the initial condition used for generating

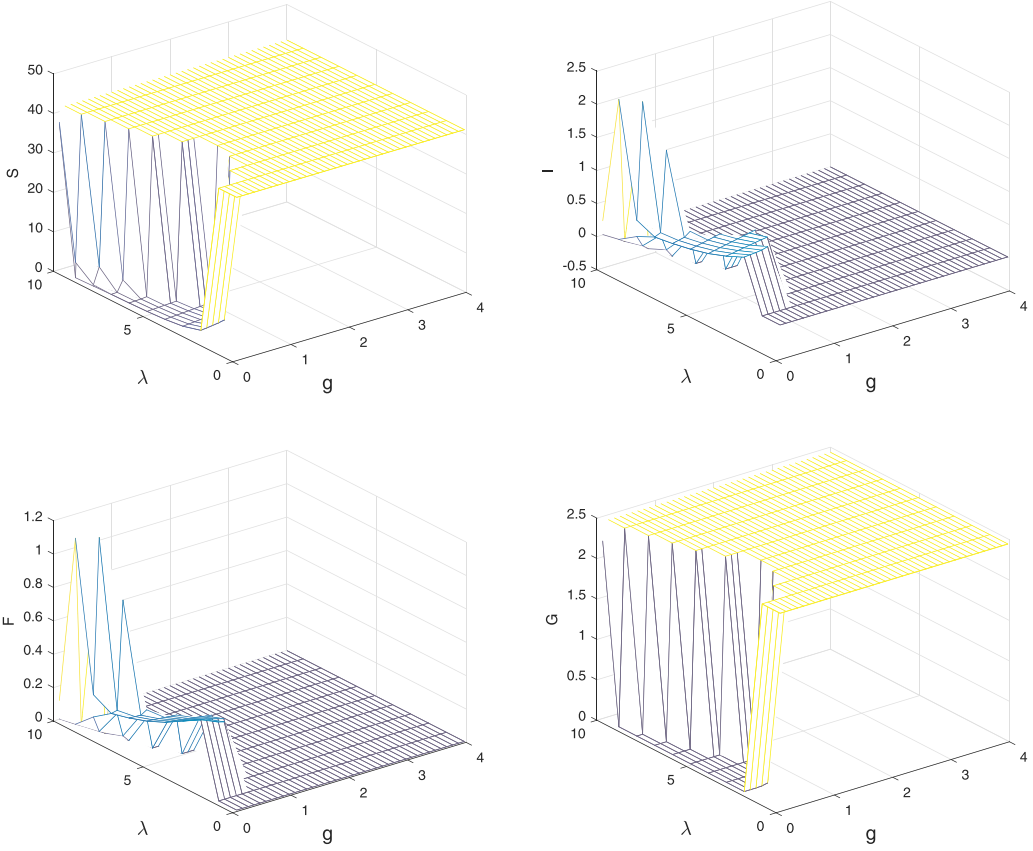

Fig. 6. The surfaces represent the population equilibrium values. Clockwise: the healthy parts of the olive tree, S, the infected parts, I, the good fungi, G and the bad fungi, F. The plots are obtained varying the parameters $g \in [0.1, 4]$ and $\lambda \in [0.1, 11]$. The initial condition is [1, 1, 1, 1].

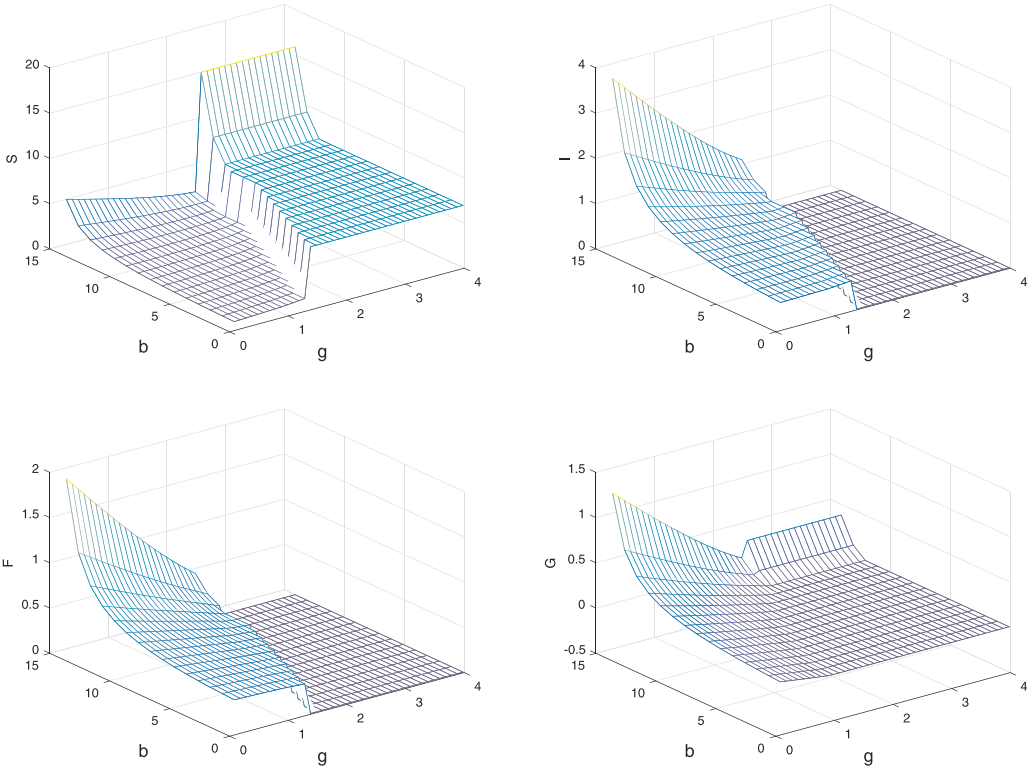

Fig. 7. The surfaces represent the population equilibrium values. Clockwise: the healthy parts of the olive tree, S, the infected parts, I, the good fungi, G and the bad fungi, F, varying the parameters $g \in [0.1, 4]$ and $b \in [0.1, 15]$. The initial condition is [1, 1, 1, 1].

the surface, namely [1,1,1,1] and of side 2. Integrating the system, only one equilibrium was found except for two cases that gave bistability between E_3 and E^*, corresponding to the parameter spaces $\lambda - q$ and $\lambda - r$. Repeating the simulation in the same way but in the hypercube of side 10, also the parameter space $\lambda - b$ shows bistability between E_3 and E^*. In Figs. 14–17 we show these previously discussed three instances and one sample for which only one equilibrium exists, namely $g - \lambda$.

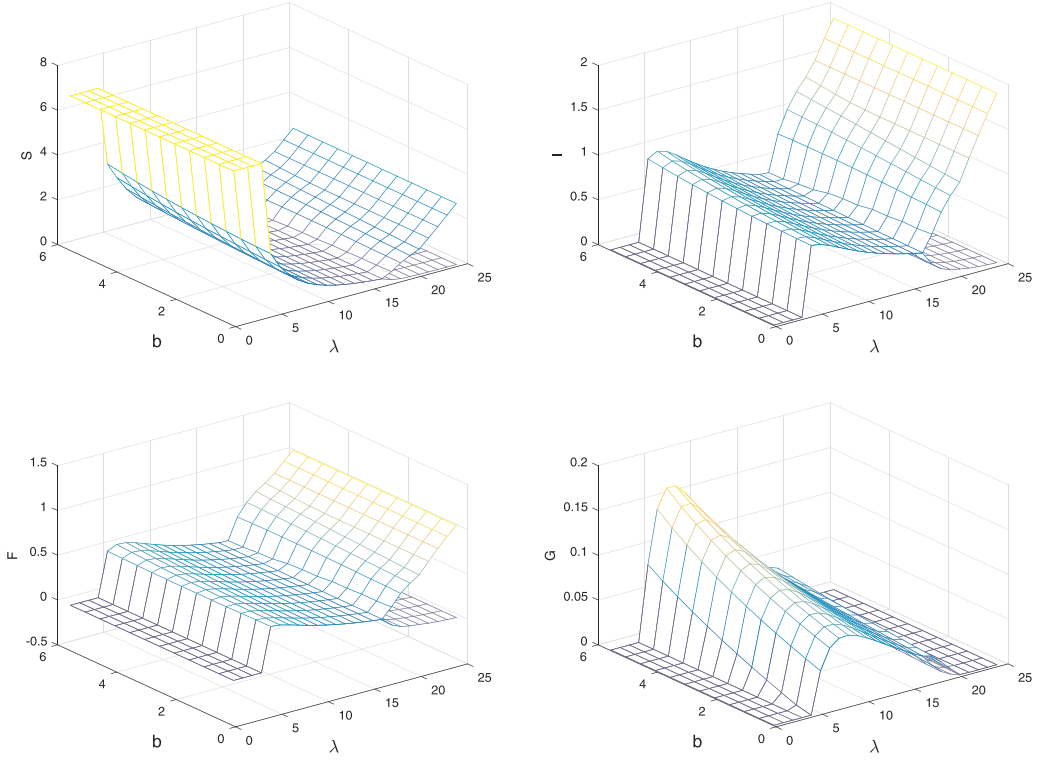

Fig. 8. The surfaces represent the population equilibrium values or the largest and smallest values of the population oscillations. Clockwise: the healthy parts of the olive tree, S, the infected parts, I, the good fungi, G and the bad fungi, F, varying the parameters $\lambda \in [0.1, 25]$ and $b \in [0.1, 6]$. The initial condition is [1, 1, 1, 1]. Persistent oscillations arise in this parameter space for high enough values of the disease transmission rate λ.

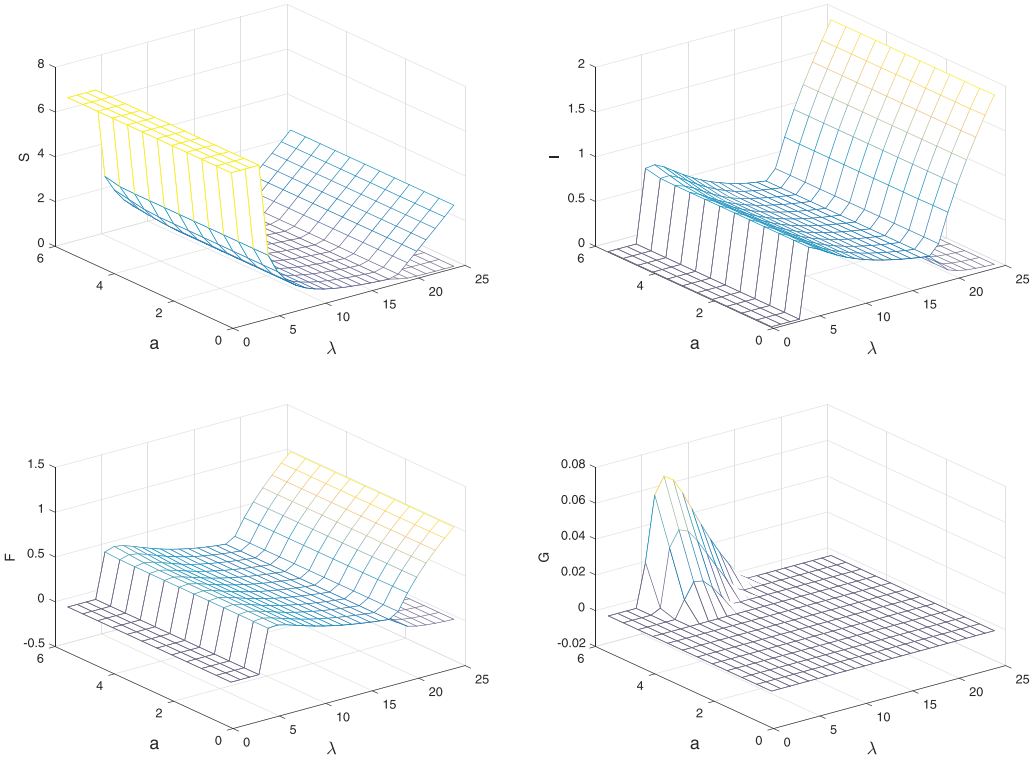

Fig. 9. The surfaces represent the population equilibrium values or the largest and smallest values of the population oscillations. Clockwise: the healthy parts of the olive tree, S, the infected parts, I, the good fungi, G and the bad fungi, F, varying the parameters $\lambda \in [0.1, 25]$ and $a \in [0.1, 30]$. The initial condition is [1, 1, 1, 1].

4.4. Biological interpretation of the simulation results

From a biological point of view it is important to know that choosing different initial conditions the ecosystem may behave in very different ways. We have seen that some of them lead the system to different stable equilibria. For instance in the case of the pair E_3 and E_2 the choice of the initial conditions influences how the disease ultimately behaves, whether is it eradicated because the trajectories

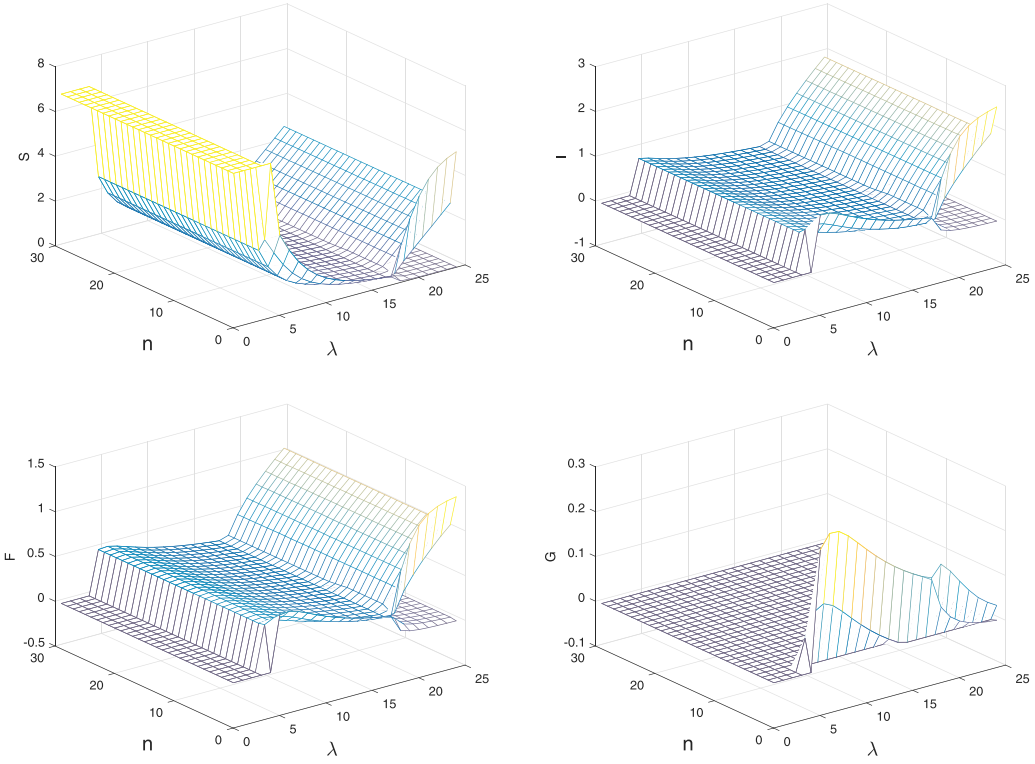

Fig. 10. The surfaces represent the population equilibrium values or the largest and smallest values of the population oscillations. Clockwise: the healthy parts of the olive tree, S, the infected parts, I, the good fungi, G and the bad fungi, F, varying the parameters $\lambda \in [0.1, 25]$ and $n \in [0.1, 30]$. Initial condition: [1, 1, 1, 1].

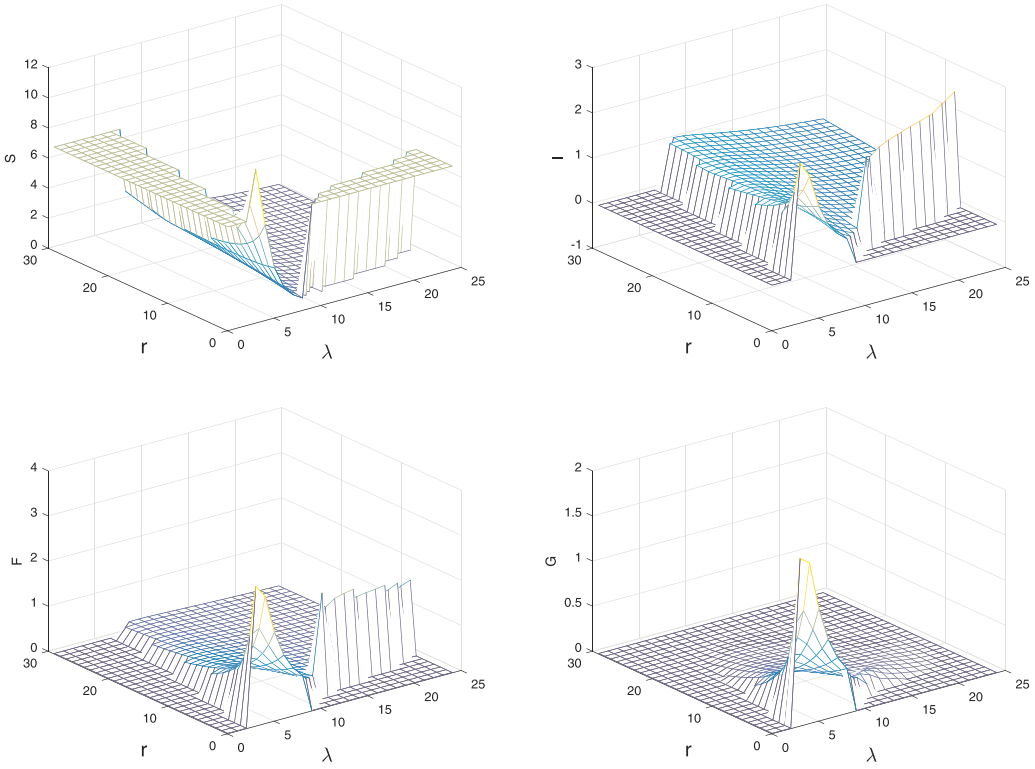

Fig. 11. The surfaces represent the population equilibrium values. Clockwise: the healthy parts of the olive tree, S, the infected parts, I, the good fungi, G and the bad fungi, F, varying the parameters $\lambda \in [0.1, 25]$ and $r \in [0.1, 30]$. The initial condition is [1, 1, 1, 1].

approach the disease-filamentous fungi-free point or it persists, if the phyllosphere microorganisms-free point is instead attained. These behaviors have clearly huge differences and economic impact. Therefore in case the ecosystem is at a situation leading to the endemic state of the disease, devising biological means to push the present state of the system into another configuration belonging to the basin of attraction of the disease-free state becomes imperative for disease eradication and regain a healthy tree environment.

For the pair of bistable equilibria E_1 and E_3 we also know the separatrix surface, thereby it is possible to assess precisely the actions to take to remove the disease. This can practically be achieved by spraying the infected tree with more phyllosphere microorganisms or

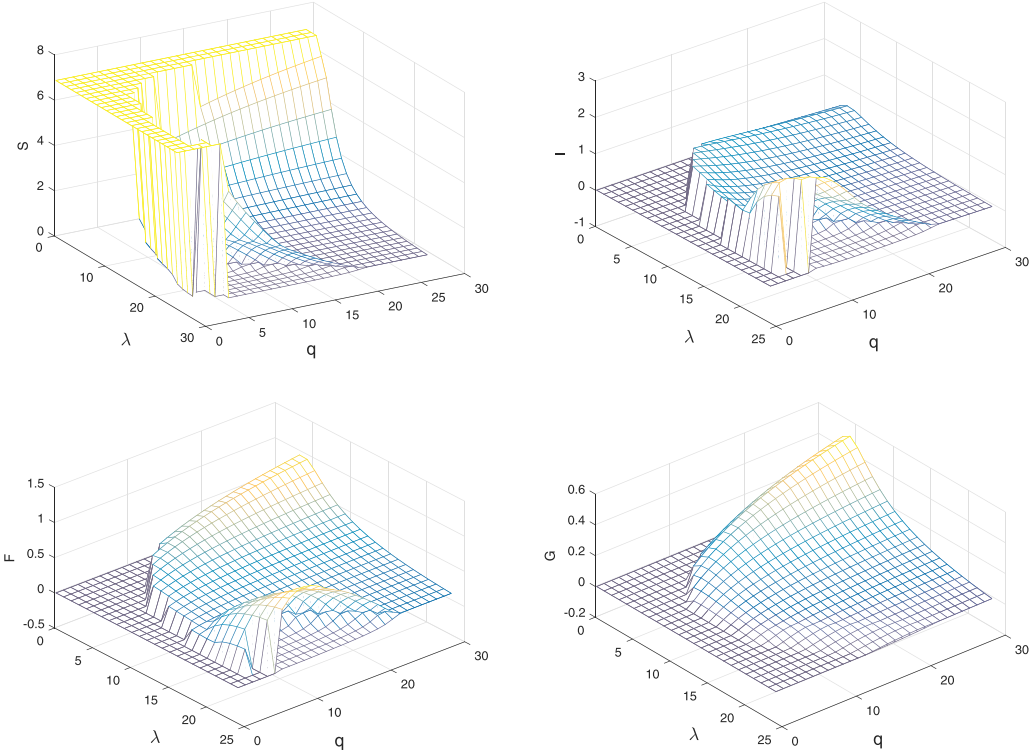

Fig. 12. The surfaces represent the population equilibrium values. Clockwise: the healthy parts of the olive tree, S, the infected parts, I, the good fungi, G and the bad fungi, F, varying the parameters $\lambda \in [0.1, 25]$ and $q \in [0.1, 30]$. The initial condition is [1, 1, 1, 1]. (Note that the axes in this frame are rotated to better show the equilibrium surfaces, so that the origin is in front and not on the left as in the other figures).

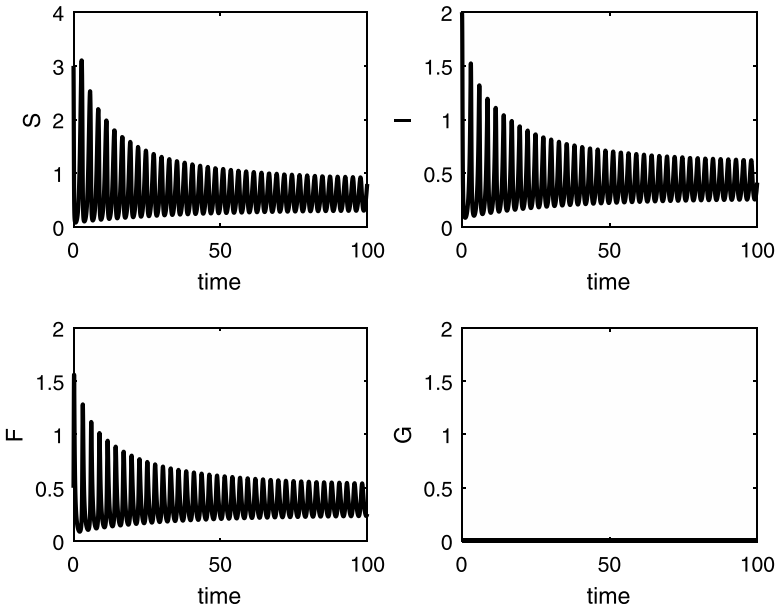

Fig. 13. The sustained oscillations around the endemic equilibrium E_3, with initial condition [1, 1, 1, 1]. Clockwise: the healthy parts of the olive tree, S, the infected parts, I, the good fungi, G and the bad fungi, F.

alternatively by pruning the infected branches. In this case a counter-intuitive result is obtained, in fact it seems that by choosing a high value of F, the filamentous fungi, and in case of high infection of the leaves I as well, and if both the healthy foliage S and the filamentous fungi F increase, the situation of a stable healthy tree can still be achieved. This result can be obtained if the carrying capacity of the olive tree foliage is suitably bounded above, see (4). This however may be difficult to obtain in the real life situations. Another more intuitive result obtained from Fig. 3, is that for a chosen set of parameters and values of F small enough the healthy tree-only point can be attained in a stable way.

From the transcritical bifurcation diagrams, Figs. 4 and 5, varying the same parameter λ, the infection rate, and for two different sets of parameters, two completely different results can be reached. Fig. 4 shows that for values of the infection rate small enough the healthy tree equilibrium is stable; increasing λ the system first experiences the disease infection, at coexistence, and finally the situation worsens up to the point where phyllosphere microorganisms are completely wiped out. From Fig. 5 instead the healthy tree configuration is stably obtained either by a low disease transmission rate, or for high enough values of the same parameter, in this case $\lambda > 10$. For intermediate values of the disease transmission rate, typically $1 < \lambda < 10$, the system attains the stable good fungi-free state, with endemic disease. Biologically this means that if the infection rate is very weak or really strong the olive tree can be freed from the disease and from the filamentous fungi too. This result makes sense: for a weak infection the phyllosphere microorganisms are able to repel the filamentous fungi invasion before they attain large values, while for a strong infection it means that the filamentous fungi will quickly exhaust the tree resources, and thereafter will not be able to survive themselves, while the tree instead is still able

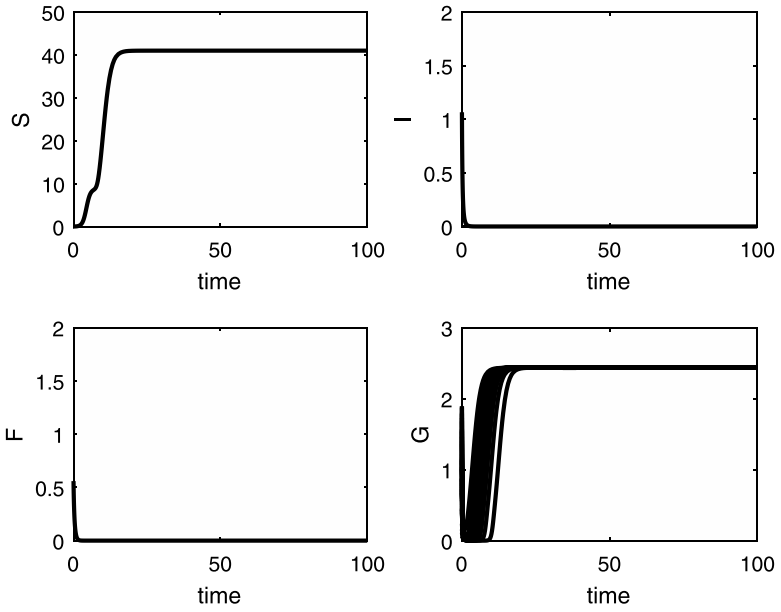

Fig. 14. Simulations with the same parameter values as of the corresponding equilibrium surface cases. The chosen parameter space is $g - \lambda$; the initial conditions are taken in the hypercube of side 10 with center [1,1,1,1].

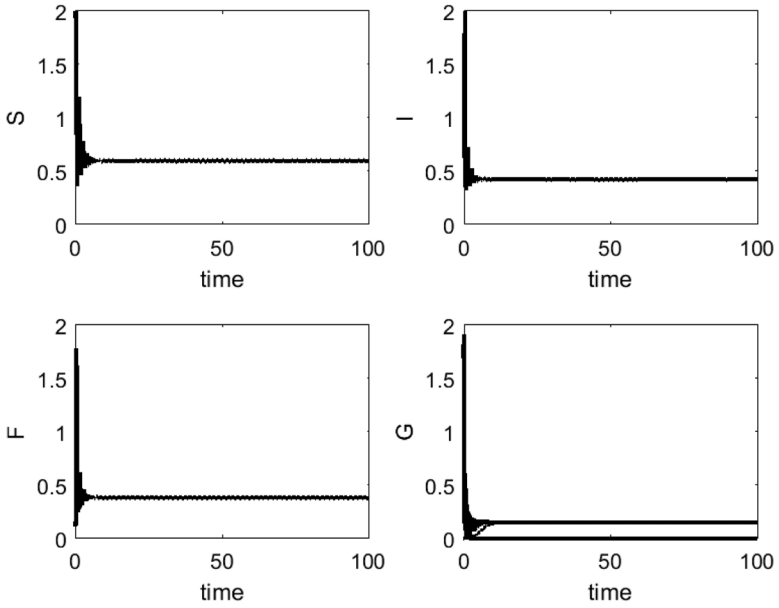

Fig. 15. Simulations with the same parameter values as of the corresponding equilibrium surface cases. The chosen parameter space is $\lambda - q$; the initial conditions are taken in the hypercube of side 10 with center [1,1,1,1].

to recover. Note indeed that a high value of the infected branches population I induces also a high reduction in the filamentous fungi population, F, for which the latter may very well be fast depleted and therefore free the tree from the infection.

It is interesting to observe that for $\lambda < 5$ in Fig. 4 the tree is healthy, while in Fig. 5 in the same range for the disease transmission, up to $\lambda > 1$, the ecosystem is still in the endemic state, while for $\lambda < 1$ the infection vanishes. Therefore the minimal threshold for disease eradication depends not only on disease transmission, but also from the remaining parameters of the model.

Several transcritical bifurcations arise the surfaces plotted in Figs. 6–11 illustrating smooth transitions among the ecosystem equilibria, depending on some of the model parameters. In addition these figures indicate that the system may also enter into a state of sustained oscillations via suitable Hopf bifurcations, indicating periods of high and low infections on the tree. This information would be important for the external treatments with fungicides, as they would result most effective during the periods of low infection. Indeed an external additional filamentous fungi human-induced mortality, administered when this population is low, could make it vanish altogether, thereby eradicating the disease.

One further point that we remark here is that the equilibrium surfaces depicted in Figs. 6–12 do not show the only possible equilibrium, as indicated by the results of the further simulations using random initial conditions. Bistability can indeed occur. In particular it involves the equilibrium E_3 in addition to coexistence, which entails the possible loss of the phyllosphere good fungi. Once more, the importance of the assessment of the separatrix between these equilibria basins of attraction is apparent. But also, in spite of the bistability, the shapes of the equilibrium surfaces should provide means of intervening to the

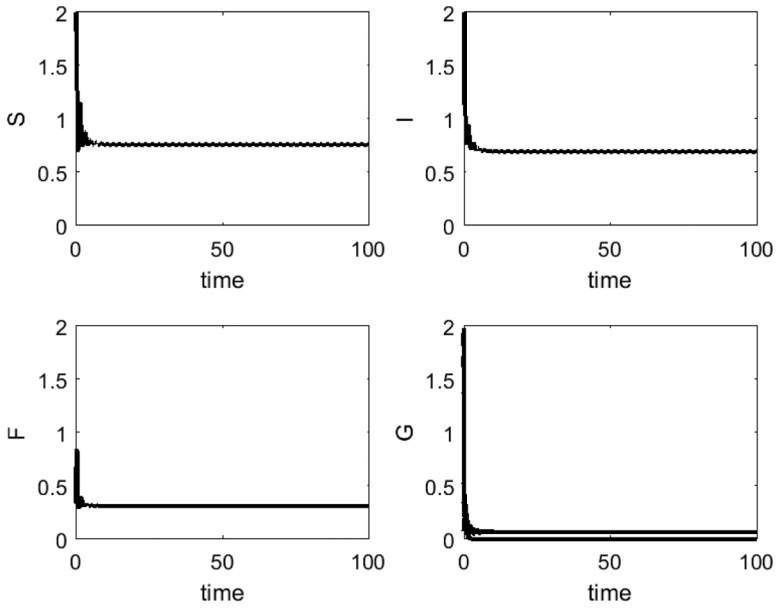

Fig. 16. Simulations with the same parameter values as of the corresponding equilibrium surface cases. The chosen parameter space is $\lambda - r$; the initial conditions are taken in the hypercube of side 10 with center [1,1,1,1].

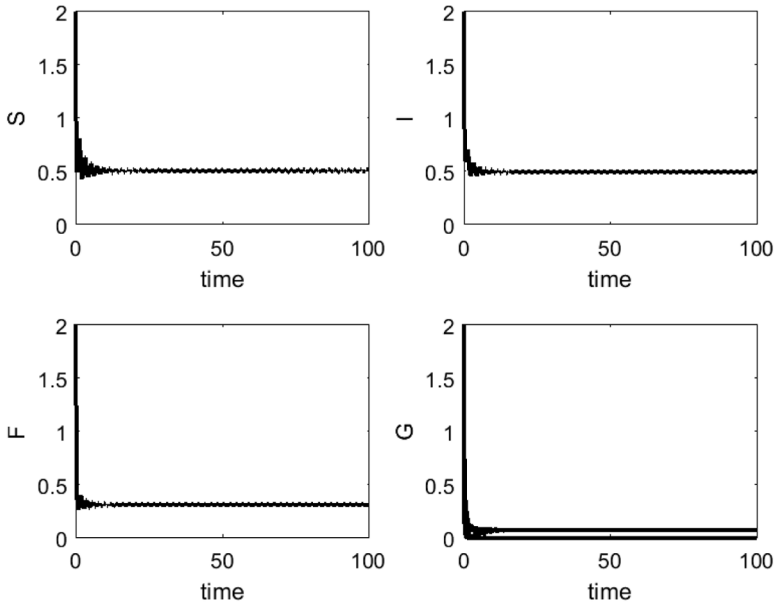

Fig. 17. Simulations with the same parameter values as of the corresponding equilibrium surface cases. The chosen parameter space is $\lambda - b$; here initial conditions are taken in the hypercube instead of side 10 with center [1,1,1,1].

ecologist that wants to control the pathogens that cause the disease outbreak. First of all, by seeking parameter configurations that contain, even at coexistence, the bad fungi and the infected branches populations at low levels. Secondly, looking for high values of the good phyllosphere microorganisms and operating on the suitable parameters accordingly. In this respect, as already mentioned in the introduction, synthesizing in the laboratory the antagonistic molecules could also provide a substantial help.

5. Conclusions

We have presented a model for disease infection and eradication of the olive tree, due to the action of two kinds of fungi, the pathogenic ones and the beneficial ones.

The findings of the analysis and simulations show that from a biological point of view the most important equilibria are E_2 healthy tree with phyllosphere microorganisms as well as E_1, the purely healthy tree. At this point indeed only the healthy olive tree thrives, with no other microorganisms in it; this is most likely impossible in the real world. At E_2 instead the healthy tree contains also the phyllosphere microorganisms, which help in repelling the possible attacks of pathogenous agents. This is a better goal to achieve, as the latter represent a natural way of fighting filamentous fungi invasions. On the other hand, the equilibrium E_3 is the most dangerous one since it corresponds to endemic disease. In it the infected parts of the tree and the invading filamentous fungi are present, while the phyllosphere microorganisms are wiped out. The qualitative analysis of the model (2) states that E_2 is feasible and stable if the carrying capacity of the olive tree, K, does not exceed a certain threshold. Our extensive numerical simulations have revealed the existence of some special cases, in which bistability of three pairs of equilibria occurs. The most important one is obtained for the set of parameters (21) for which E_2 and E_3 are both stable. Thus starting from different initial conditions the system can respectively either be freed from the disease, or invaded by the filamentous fungi. A way to force the ecosystem to attain a state belonging to the right basin of attraction, the one of the healthy tree configuration, would in practice be implemented by using pruning, thus simultaneously reducing the amounts of the infected foliage and of the filamentous fungi respectively. Note indeed that in the model g represents disease-related mortality, but with a wider interpretation it can become a control parameter, represented indeed by pruning. If applied with a high measure, it can effectively contribute to disease eradication, as indicated by our numerical experiments. Here it is seen once more the importance of keeping the various mortality terms distinct from each other in the model formulation, as it is just one of them that we need to use for the benefit of the tree. A complementary or alternative measure could be given by adding more phyllosphere microorganisms to the olive tree. This can be achieved by sythesizing in the laboratory the antagonistic molecules that they produce, and then spray them on the tree.

In addition we have discovered that E_1 can be stable together with E_3 or E^* respectively. E_1 is the equilibrium where only the healthy parts of the olive tree thrive while in the other two, E^* being the coexistence equilibrium, invasion of the filamentous fungi occurs, in spite of the presence of the phyllosphere microorganisms.

Further important information arises from the Figs. 6–8. In particular keeping the same initial conditions, thus assuming that no pruning or adding good fungi is performed, the values of a pair of two parameters of the model are simultaneously changed. In Fig. 6 varying λ, the infection rate, and g, the mortality rate of the infected parts, two different equilibrium points can be attained, E_2 or E_3. The same occurs in Fig. 7, with the equilibria E^* or E_1. Furthermore Figs. 8–11 show that the system may present sustained oscillations for values of λ greater than 18. As previously remarked, an application of fungicides at the throughs of these oscillations may wipe out the filamentous fungi and thereby free the tree from the infection.

From the more applied side, what happens in reality is not really known, because of the difficulty of studying such microbial interactions in the phyllosphere. Thus, data about the effect of the application of microorganims on olive tree leaves under natural conditions are lacking. There are several reasons for this missing information. The data obtained in the field situation are quite different from the response that can be gathered in the laboratory under very carefully designed side conditions. First of all, the pathogens are indeed very resistant to being cultivated in vitro. Moreover, as mentioned in the introduction, it is indeed very difficult if not impossible to investigate this situation in the open environment, as the trees must be sterilized, before starting the experiments to assess what happens on the real leaves, and kept so, otherwise the other microorganisms present in the phyllosphere may alter the experiments results. Even to the biologists in our team then,

this mathematical model appears to be if not the best way, at least a very useful tool that allows at least a qualitative mean of investigation for providing speculative information on the interactions that can arise between the pathogen and beneficial fungi.

Acknowledgements

EV and IMB have been partially supported by the projects “Metodi numerici in teoria delle popolazioni” and “Metodi numerici nelle scienze applicate” of the Dipartimento di Matematica “Giuseppe Peano” of the Università di Torino. IMB has been partially supported by ”Finanziamento GNCS Giovani Ricercatori 2016”.

Appendix A

Analysis of model (3).

Proposition 1.

(i) *The trivial equilibrium point* $E_0 = (0, 0)$ *is always feasible but unstable.*
(ii) *The good fungi-free point* $E_1 = (K, 0)$ *is always feasible and is stable if the carrying capacity of S is suitably bounded from above, as stated in (4).*
(iii) *The coexistence equilibrium point* E_2*, where the tree is healthy and the phyllosphere microorganisms thrive in it, (5) is feasible if either one of the two alternative sets (6) or (7) holds.*
Stability of E_2 *is given by Eq. (8).*

Proof. The equilibrium points are easily obtained from the corresponding equilibrium equations of (3). For the study of their stability we need the Jacobian of (3):

$$J = \begin{bmatrix} -\frac{sS}{K} + s\left(1 - \frac{S}{K}\right) + bG & bS \\ beG - \frac{sG}{K} & beS - 2pG - n - \frac{sS}{K} \end{bmatrix} \tag{A.1}$$

evaluates at each equilibrium point. Specifically:

(i) E_0 is a trivial solution of the homogeneous system; it is unstable, in view of the Jacobian eigenvalues $-n < 0$ and $s > 0$.
(ii) For $G = 0$ the first equilibrium equation of (3) gives $S = K$. The Jacobian's eigenvalues are $-s < 0$ and $Kbe - n - s$, from which the stability condition (4) follows.
(iii) Solving the equilibrium system for nonvanishing populations provides the coexistence point (5), which is feasible if the populations are non-negative, giving the alternative conditions

$$n \le \frac{ps}{b}, \quad \frac{n+s}{be} \le K < s\frac{b+p}{b^2e}, \quad n \ge \frac{ps}{b}, \quad \frac{n+s}{be} \ge K > s\frac{b+p}{b^2e},$$

from which (6) and (7) follow. Using the equilibrium equations, the diagonal entries of the Jacobian in this case simplify:

$$J_{11} = -s\frac{S_2}{K}, \quad J_{22} = -pG_2.$$

Hence, using the Routh–Hurwitz conditions,

$$-\operatorname{tr}(J(E_2)) > 0, \quad \det(J(E_2)) = S_2G_2\left[p\frac{s}{K} - b\left(be - \frac{s}{K}\right)\right].$$

The latter is positive whenever (8) holds. If follows that the feasibility conditions (7) are incompatible with the stability requirement.

□

Appendix B

Here we provide some details of the analysis of the model (9). The Jacobian matrix of (9) is

$$J = \begin{bmatrix} J_{11} & -\frac{sS}{K} & -\lambda S \\ \lambda F - \frac{s}{K}I & J_{22} & \lambda S - qI \\ -\frac{sF}{K} & hqF - \frac{sF}{K} & J_{33} \end{bmatrix} \tag{B.1}$$

with

$$J_{11} = s - 2\frac{sS}{K} - \frac{sI}{K} - \lambda F, \quad J_{22} = -qF - g - \frac{sS}{K} - 2\frac{sI}{K},$$
$$J_{33} = hqI - m - 2rF - g - s\frac{S+I}{K}. \tag{B.2}$$

For the origin, the instability follows as in the former model by the positive eigenvalue s, while the other ones are $-g$ and $-g-m$.

The healthy branches-only point E_1, contrary to the case of the (S, G) model, in this case possesses the eigenvalues $-s$, $-g-s$ and $-m-g-s$. Since they are all negative, its unconditional stability follows.

Proposition 2. *The population values at coexistence equilibrium of model (9) are given in (10). F_3 is the positive root of the quadratic equation*

$$\psi(F) := UF^2 + VF + Z = 0, \qquad U = \frac{q}{s}[s(\lambda - r) - hK\lambda^2],$$
$$V = qh\lambda K - q(m+g+s) + (\lambda - r)(g+s), \quad Z = -(s+g)(m+g+s) < 0. \tag{B.3}$$

The conditions for exactly one and two such roots are respectively

$$U > 0; \qquad U < 0, \quad V > 0, \quad V^2 \geq 4UZ. \tag{B.4}$$

In addition, further feasibility conditions are (11). Stability hinges on the Routh–Hurwitz conditions for a cubic polynomial, that are indicated in the proof.

Proof. The coexistence equilibrium is obtained by solving the first equation of (9) with respect to S and then substituting it into the second and third equations respectively. The last equation provides I, and its substitution into the second one gives the quadratic equation in F, (B.3) Since $\psi(0) < 0$, one positive root exists if the first condition in (B.4) holds. Instead, to have two, the second set of conditions (B.4) must be satisfied. Feasibility conditions hinges further on the nonnegativity of the remaining populations, (11). The case $U < 0$, $V > 0$, $V^2 < 4UZ$ instead does not give any equilibrium point of this type.

Note that at coexistence the diagonal entries (B.2) of the Jacobian simplify to

$$J_{11} = -\frac{sS}{K}, \quad J_{22} = -\frac{\lambda SF}{I} - \frac{sI}{K}, \quad J_{33} = -rF.$$

Thus for stability of E_3 the eigenvalues of $J|_{E_3}$ are the roots of the cubic equation $\mu^3 + R_1\mu^2 + R_2\mu + R_3 = 0$ with

$$\begin{aligned}
R_1 &= (F_3 I_3 Kr + F_3 K S_3 \lambda + F_3^2 s + I_3 S_3 s)(KI_3)^{-1} > 0\\
R_2 &= (F_3 I_3^2 Khq^2 - F_3 I_3 K S_3 h\lambda\, q + F_3^2 K S_3 \lambda\, r - F_3 I_3^2 qs + F_3 I_3^2 rs\\
&\quad + F_3 I_3 S_3 \lambda\, s + F_3 I_3 S_3 rs + F_3 S_3^2 \lambda\, s)(KI_3)^{-1}\\
R_3 &= (F_3^2 I_3 K S_3 h\lambda^2 q - F_3 I_3^2 S_3 h\lambda\, qs + F_3 I_3^2 S_3 hq^2 s - F_3 I_3 S_3^2 h\lambda\, qs\\
&\quad + F_3^2 I_3 S_3 \lambda\, rs - F_3^2 I_3 S_3 \lambda^2 s - F_3^2 S_3^2 \lambda^2 s + F_3^2 S_3^2 \lambda\, rs)(KI_3)^{-1}
\end{aligned} \tag{B.5}$$

Now, $R_1 > 0$ while the signs of R_2 and R_3 depend on the parameters values. If $0 < R_3 < R_1 R_2$ then E_3 is stable. Explicitly this condition becomes:

$$\begin{aligned}
R_1 R_2 - R_3 &= F_3 I_3^3 K^2 hq^2 r + F_3 I_3^2 K^2 S_3 h\lambda\, q^2 - F_3 I_3^2 K^2 S_3 h\lambda\, qr\\
&\quad + F_3^2 I_3 K^2 S_3 \lambda\, r^2 + F_3^2 K^2 S_3^2 \lambda^2 r + I_3^4 Khq^2 s + F_3 I_3 S\lambda^2 s\\
&\quad + I_3^3 K S_3 hq^2 s - I_3^2 K S_3^2 h\lambda\, qs - F_3 I_3^3 Kqrs + F_3 I_3^3 Kr^2 s\\
&\quad - F_3 I_3^2 K S_3 \lambda\, qs + 3 F_3 I_3^2 K S_3 \lambda\, rs + F_3 I_3^2 K S_3 r^2 s\\
&\quad + 3 F_3 I_3 K S_3^2 \lambda\, rs - F_3 I_3 K S_3 h\lambda^2 q + F_3 K S^3 \lambda^2 s - I_3^4 qs^2\\
&\quad + I_3^3 S_3 \lambda\, s^2 - I_3^3 S_3 qs^2 + 2 I_3^3 S_3 rs^2 + 2 I_3^2 S_3^2 \lambda\, s^2\\
&\quad + I_3^2 S_3 h\lambda\, qs - I_3^2 S_3 hq^2 s + I_3 S_3^3 \lambda\, s^2 + I_3 S_3^2 h\lambda\, qs\\
&\quad - F_3 I_3 S_3 \lambda\, rs + F_3 S_3^2 \lambda^2 s - F_3 S_3^2 \lambda\, rs + I_3^2 S_3^2 rs^2\\
&\quad + F_3 I_3 K S_3^2 \lambda^2 s - F_3 I_3 K^2 S_3^2 h\lambda^2 q + I_3^4 rs^2 - I_3^3 K S_3 h\lambda\, qs.
\end{aligned}$$

□

Appendix C

Analysis of model (2).

Proposition 2. *Assuming to have two feasible values for S_* and I_* (it was shown numerically that a set of parameters exists for which $S_* > 0$ and $I_* > 0$), the coexistence equilibrium*

$$E_* = \left(S_*, I_*, F_*, \frac{F_* K\lambda + I_* s - Ks + S_* s}{Kb}\right),$$

with

$$F_* = \frac{I_* Kbhq - I_* as - I_* bs + Kas - Kbg - Kbm - S_* as - S_* bs}{(a\lambda + br)K} \tag{C.1}$$

is stable if the Routh–Hurwitz conditions

$$P_3 > 0, \quad P_4 > 0, \quad P_1 P_2 P_3 > P_3^3 + P_1^2 P_4, \tag{C.2}$$

hold.

Proof. The coexistence equilibrium E_* is obtained following the next steps:

- Step 1: Solve for G the first equation of (2) to get G_*, (18).
- Step 2: Substitute G obtained in Step 1 into the third equation of (2) to get F_*, (19).
- Step 3: Evaluate the second and the fourth equations using the values F_* and G_* from Steps 1 and 2, to get

$$H(S, I) = A_1 I^2 + A_2 I + A_3 = 0$$

with A_1, A_2 and A_3 defined as follows

$$\begin{aligned} A_1 &= (((q - r)s - Khq^2)b - sa(\lambda - q)) \\ A_2 &= ((-S(\lambda - q + r)s + K(\lambda Shq + (g + m)q - gr))b \\ &\quad - ((2\lambda S + q(K - S))s + K\lambda g)a) \\ A_3 &= ((-Ss - K(g + m))b + sa(K - S))\lambda S \end{aligned} \tag{C.3}$$

and

$$M(S, I) = B_1 S^3 + B_2 S^2 + B_3 S + B_4$$

with B_1, B_2, B_3 and B_4 defined as follows

$$\begin{aligned} B_1 &= (-be(a\lambda + br)K + s((-p + a)\lambda + ua^2 + uab + \\ &\quad r(b + p)))s(r - \lambda) \\ B_2 &= (((((-abe + hpq)\lambda - quabh - rb^2e)K + 2s((-p + a)\lambda + ua^2 + \\ &\quad uab + r(b + p)))I - ((a^2u + pr)s + (-na + p(g + m))\lambda - \\ &\quad b(u(g + m)a + rn))K)s(r - \lambda) + (-be(a\lambda + br)K + s((-p + a)\lambda + \\ &\quad ua^2 + uab + r(b + p)))((Kq\lambda h + s(r - \lambda))I + (-sr - \lambda(g + m))K)) \\ B_3 &= (((qh(-abu + \lambda p)K + s((-p + a)\lambda + ua^2 + uab + r(b + p)))I^2 + \\ &\quad ((-a^2u - pr)s + ((g + n)a - p(g + m))\lambda + (u(g + m)a + \\ &\quad r(g + n))b)KI)s(r - \lambda) + ((((-abe + hpq)\lambda - quabh - rb^2e)K + \\ &\quad 2s((-p + a)\ lambda + ua^2 + uab + r(b + p)))I - ((a^2u + pr)s + \\ &\quad (-na + p(g + m))\lambda - b(u(g + m)a + rn))K)((Kq\lambda h + \\ &\quad s(r - \lambda))I + (-sr - \lambda(g + m))K)) \\ B_4 &= ((qh(-abu + \lambda p)K + s((-p + a)\lambda + ua^2 + uab + r(b + p)))I^2 + \\ &\quad ((-a^2u - pr)s + ((g + n)a - p(g + m))\lambda + (u(g + m)a + \\ &\quad r(g + n))b)KI)((Kq\lambda h + s(r - \lambda))I + (-sr - \lambda(g + m))K). \end{aligned} \tag{C.4}$$

- Step 4: The intersection of these curves $H(S, I)$ and $M(S, I)$ provides the values of the remaining populations, S_* ,I_*.

The Jacobian of (2) is

$$J = \begin{bmatrix} J_{11} & -\frac{sS}{K} & -\lambda S & bS \\ \lambda F - \frac{sI}{K} & J_{22} & \lambda S - qI & 0 \\ -\frac{sF}{K} & hqF - \frac{sF}{K} & J_{33} & -aF \\ beG + \frac{gGI}{(S+I)^2} - \frac{sG}{K} & -\frac{gG}{(S+I)} + \frac{gGI}{(S+I)^2} & uaG & J_{44} \end{bmatrix}. \tag{C.5}$$

with

$$J_{11} = s - 2s\frac{S}{K} - s\frac{I}{K} - \lambda F + bG, \quad J_{22} = -qF - g - 2s\frac{I}{K} - \frac{sS}{K},$$
$$J_{33} = hqI - aG - m - 2rF - g - s\frac{S+I}{K},$$
$$J_{44} = ebS + uaF - n - 2pG - g\frac{I}{S+I} - s\frac{S+I}{K}$$

Now at the origin one eigenvalue is $s > 0$ showing its instability. At E_1, they are $-s, -g-s, -g-m-s, -n-s$, so that this point remains unconditionally stable also in the enlarged four-dimensional phase space. For E_2, we find the eigenvalues of the $S - G$ subsystem and in addition the negative ones

$$-g - s\frac{S_2}{K}, \quad -aG_2 - m - g - s\frac{S_2}{K},$$

which do not alter the stability of this equilibrium obtained in the $S - G$ subsystem. Finally for E_3, the phyllosphere microorganisms-free point, corresponding to the coexistence equilibrium of the $S - I - F$ subsystem, there is one additional eigenvalue, J_{44}, which provides the additional stability condition (17).

To study the stability of the coexistence equilibrium we evaluate (C.5) at E^*. Note the simplifications in the diagonal entries: $J_{33}(E^*) = -rF^*$, $J_{44}(E^*) = -pG^*$ and

$$J_{11}(E^*) = -\frac{sS^*}{K}, \quad J_{22}(E^*) = -\frac{\lambda S^* F^*}{I^*} - \frac{sI^*}{K}.$$

Stability of the equilibrium E^* can be studied, at least in principle, by assessing the positive definiteness of $-J(E^*)$. Now $-J_{11} > 0$, while the principal minor of order 2 provides already the stability condition

$$\frac{\lambda S^* F^*}{I^*} + \frac{sI^*}{K} + \lambda F^* > \frac{sI^*}{K} \tag{C.6}$$

The principal minor of order 3 is actually $-R_3$ given in (B.5). Finally the positivity of $-\det(J(E^*))$ must be ensured.

Alternatively, the Routh–Hurwitz conditions (C.2) can be used, where the above quantities are the coefficients of the characteristic polynomial of $J(E^*)$,

$$\mu^4 + P_1\mu^3 + P_2\mu^2 + P_3\mu + P_4.$$

□

References

[1] A. Loumou, C. Giourga, Olive groves: the life and identity of the mediterranean, Agricult. Hum. Values 20 (2003) 87–95.

[2] P. Malcolm, History of Olive Trees, (2006). http://EzineArticles.com/368070 - November 24, 2006

[3] D. Barranco, R. Fernández-Escobar, L. Rallo, El cultivo del olivo, 7a edicion, Ediciones Mundi-Prensa, Spain, 2017.

[4] C. Malavolta, D. Perdikis, IOBC technical guidelines III. Guidelines for integrated production of olives, IOBC/WPRS Bull. 77 (2012) 1–19.

[5] J.A. Vorholt, Microbial life in the phyllosphere, Nat. Rev. Microbiol. 10 (2012) 828–840.

[6] M.L. Friesen, S.S. Porter, S.C. Stark, E.J. von Wettberg, J.L. Sachs, E. Martinez-Romero, Microbially mediated plant functional traits, Annu. Rev. Ecol. Evol. Syst 42 (2011) 23–46.

[7] L.P. Partida-Martnez, M. Heil, The microbe-free plant: fact or artifact? Front. Plant Sci. 2 (2011) 1–16.

[8] P.T. Lacava, J.L. Azevedo, Biological control of insect-pest and diseases by endophytes, in: V.C. V. Verma, A.C. Gange (Eds.), Advances in Endophytic Research Part, Springer, India, 2014, pp. 231–256.

[9] S.W. Kembel, T.K. O'Connor, H.K. Arnold, S.P. Hubbell, S.J. Wright, J.L. Green, Relationships between phyllosphere bacterial communities and plant functional traits in a neotropical forest, PNAS 111 (2014) 13715–13720.

[10] F.D. Andreote, T. Gumiere, A. Durrer, Exploring interactions of plant microbiomes, Sci. Agric. 71 (2014) 528–539.

[11] A. Sessitsch, B. Mitter, 21st century agriculture: integration of plant microbiomes for improved crop production and food security, Microb. Biotechnol. 8 (2015) 32–33.

[12] K. Jacobsen, J. Stupiansky, S.S. Pilyugin, Mathematical modeling of citrus groves infected by huanglongbing, Math. Biosci. Eng. 10 (3) (2013). 705–28

[13] M.A. Khan, K. Ali, E. Bonyah, K.O. Okosun, S. Islam, A. Khan, Mathematical modeling and stability analysis of pine wilt disease with optimal control, Sci. Rep. 7 (2017) 3115.

[14] Understanding the Dynamics of Emerging and Re-emerging Infectious Diseases Using Mathematical Model, in: S. Mushayabasa, C.P. Bhunu (Eds.), 2012. 91–104, 978-81-7895-549-0

[15] Y. Mammeri, J.B. Burie, M. Langlais, A. Calonnec, How changes in the dynamic of crop susceptibility and cultural practices can be used to better control the spread of a fungal pathogen at the plot scale? Ecol. Modell. 209 (2014) 178–191.

[16] J.B. Burie, A. Ducrot, A field scale model for the spread of fungal diseases in crops: the example of a powdery mildew epidemic over a large vineyard, Math. Methods Appl. Sci. 38 (2015) 3720–3737.

[17] R. Cavoretto, A. De Rossi, E. Perracchione, E. Venturino, Robust approximation algorithms for the detection of attraction basins in dynamical systems, J. Sci. Comput. 68 (2016) 395–415, https://doi.org/10.1007/s10915-015-0143-z.

[18] R. Cavoretto, A. De Rossi, E. Perracchione, Efficient computation of partition of unity interpolants through a block-based searching technique, Comput. Math. Appl. 71 (2016) 2568–2584.

[19] R. Cavoretto, A. De Rossi, E. Perracchione, E. Venturino, Reliable approximation of separatrix manifolds in competition models with safety niches, Int. J. Comput. Math. 92 (2015) 1826–1837.

[20] R. Cavoretto, A. De Rossi, E. Perracchione, E. Venturino, Graphical representation of separatrices of attraction basins in two and three dimensional dynamical systems, Int. J. Comput. Methods 14 (2017) 16. 1750008

[21] C. Berardo, I.M. Bulai, E. Venturino, P. Baptista, T. Gomes, Modeling the Endophytic Fungus *Epicoccum nigrum* Action to Fight the "Olive Knot" Disease Caused by *Pseudomonas savastanoi* pv. *savastanoi (Psv)* Bacteria in *Olea europaea* L. Trees, in: R. Mondaini (Ed.), Trends in Biomathematics: Modeling, Optimization and Computational Problems, Springer, Cham, 2018.